Adsorption of collagen-like peptides onto gold nanosurfaces

Ming Tang[a], Neha S. Gandhi[b], Kevin Burrage[b,c], and YuanTong Gu[a]*

[a] *School of Chemistry Physics and Mechanical Engineering, Queensland University of Technology, Brisbane, Australia*

[b] *School of Mathematical Sciences and [c]ARC Centre of Excellence for Mathematical and Statistical Frontiers, Queensland University of Technology – Brisbane 4001 – Australia*

Corresponding author: yuantong.gu@qut.edu.au
Professor YuanTong Gu

Abstract

The molecular behaviour of proteins in the presence of inorganic surfaces is of fundamental biological significance. Examples include ECM proteins interacting with gold nanoparticles (AuNPs) and metallic implant biomaterials such as titanium and stainless steels. The uncharged inorganic surfaces that interact strongly with the solution phase (hydrophilic surfaces) have been commonly used in disease treatments. A deep understanding of the molecular behaviour of body proteins under the presence of hydrophilic surfaces is important in terms of clinical applications. However, the adsorption mechanism of proteins onto hydrophilic surfaces remains not fully understood. Here, comprehensive molecular dynamics (MD) simulations have been carried out to study the molecular response of a human collagen molecule segment (CMS) to the presence of a planar gold surface (AuNS) in explicit solvent, aiming to unravel the adsorption mechanism of proteins onto hydrophilic surfaces. The results demonstrate that under the presence of AuNS, the CMS first biasedly diffuses towards AuNS, followed by anchoring to the gold surface, and finally stepwise adsorbs onto AuNS, where the protein adjusts its structure to maximize the interaction with AuNS. We conclude that adsorption of proteins onto hydrophilic surfaces adheres to three steps, namely, biased diffusion, anchoring and stepwise adsorption accompanied by structural adaptation. The obtained adsorption mechanism provides insights into the development of inorganic surfaces for biomedical and therapeutic applications.

Keywords: Adsorption mechanism; Collagen; Gold nanosurfaces; Molecular dynamics simulation; Protein adsorption, Hydrophilic inorganic surfaces

Introduction

The interaction between proteins and solid surfaces commonly exists in nature and science. For example, collagen-hydroxyapatite interplay plays a crucial role in biomineralization, which is an essential process for the formation of mineralized tissues such as bone. Applications of protein-surface interactions can be dated back to ancient times. Examples include gold crowns used as dental prosthetics date back to the ancient Etruscan civilization [1], and man-made nanoparticles as pigments for cosmetics by the ancient Romans [2]. In recent decades, the scope of protein-surface interactions has enlarged, due to the development of science and bionanotechnology. Metals such as titanium and stainless steels have been extensively used as biomaterials for bone replacement, due to their superior mechanical performances, such as high elastic modulus and strong resistance of fatigue [3]. Apart from involving in the surgical treatment of abnormal tissues using metallic implant biomaterials, protein-inorganic surface interactions have been commonly applied in bionanotechnology for biomedical and therapeutic applications [4]. For instance, the interaction between proteins and graphene with great structural and mechanical properties have been widely studied for bionanotechnological applications, such as biosensors [5]. In the field of diagnostics and therapeutics, nanoparticles have been commonly applied as microfluidic point-of-care devices [6] and drug carriers to enhance the delivery of drugs [7]. Hence, a thorough understanding of detailed interactions between proteins and solid surfaces at the molecular level is crucial.

Due to the widespread phenomenon of protein-surface interactions, a large amount of experiment research have been conducted to investigate the interactions between proteins and solid surfaces, using various experimental techniques. Specifically, Circular dichroism (CD) together with probes of thermal stability was employed to capture changes in the secondary structure of bovine serum albumin (BSA) due to thermal denaturation [8]. Furthermore, solid-state nuclear magnetic resonance (NMR) techniques were applied to characterize the high-resolution structure and dynamics of a hydrated biomineralization protein (statherin) adsorbed onto hydroxyapatite [9]. In addition, nanoscale imaging techniques such as atomic force microscopy (AFM) have been used to explore the interactions of solid surfaces with biomolecules such as lysozyme [10], ferritin [11], and insulin.

Despite such great experimental effort devoted to study protein-surface interactions, a detailed mechanistic understanding of the underlying physio-chemical principles remains lacking, due to

the technical limitations of experiments [12]. As powerful complementary tools of experimental techniques, computational methods have been extensively applied to explore the molecular-level mechanisms of protein-surface interactions, such as density functional theory (DFT) calculations, coarse-grained Monte Carlo simulations, and MD simulations [13]. Amongst these computational methods, full-atom MD simulations, with the best balance between accuracy and computational feasibility, are the main tool for characterizing the interactions of AuNS with amino acids [14-17], peptides [18-26] and proteins [27-29]. Specifically, MD simulations of peptides adsorption on AuNS revealed that the adsorption energy of a peptide on a certain gold surface is higher (less below zero) than the sum of the adsorption energy of its constituent amino acids on the surface, where the fraction is intimately related to the flexibility of the peptide [19, 21-23, 25]. In addition, the adsorption process is found to be closely modulated by the flexibility of the biomolecules [18, 19, 21-23, 25, 29-31].

Despite the great importance of interactions between proteins and the uncharged hydrophilic surfaces, very few studies have been performed to understand the adsorption mechanism of proteins onto those surfaces. Until now, only one MD simulation study [32] investigated the molecular behaviours of the A3 peptide and the SD152 peptide under the presence of the Au(1 1 1) surface and the Pt(1 1 1) surface, respectively, focusing on unravelling the adsorption mechanism of peptides onto the uncharged hydrophilic surfaces. This work proposed a three-stage adsorption mechanism of biomolecules onto hydrophilic surfaces, i.e., biased diffusion phase, anchoring phase and lockdown phase. However, as the complex cooperative behaviour of proteins can remarkably alter their adsorption properties, the adsorption behaviours of proteins onto hydrophilic surfaces may differ from those reported for small peptides [32]. Motivated by this knowledge gap, this study investigates the molecular behaviour of a collagen triple helix (CMS) under the presence of AuNS in explicit water using MD simulations, aiming to explore the adsorption mechanism of proteins onto neutral hydrophilic surfaces at the molecular level. Our results yield a general three-step adsorption mechanism for proteins onto uncharged hydrophilic surfaces, and demonstrate that the CMS forms a rapid association and strong interactions with AuNS, resulting in a severe unfolding of its triple-helical structure.

Computational models and method

Model building

The Triple Helical collagen Building Script (THeBuScr) [33] was employed to build the CMS. The CMS peptides adopt the following sequences (numbers indicate residue numbers of the first and last amino acids along the sequences): $_{2,66}$GARGLPGTAGLPGM**K**GHRGFSGLDGAKGDA$_{31,95}$ (for chain A and chain C, respectively), and $_{34}$GARGFPGTPGLPGF**K**GIRGHNGLDGLKGQP$_{63}$ (for chain B). These amino acid sequences are taken from the sequences of human type I collagen (PubMed entry number NP_000079 for α1 chains, and NP_000080 for α2 chain). The N-termini and C-termini of each peptide were capped with Ace and Nme residues, respectively, so as to eliminate artefacts induced by charges at both ends. Consequently, each chain is composed of ten Gly-X-Y triplets plus two terminal residues (chain A, B, and C contain residues 1-32, 33-64, and 65-96, respectively). This leads to a CMS carrying a length of around 92 Å. Adsorption of collagen triple helices with similar length has been studied in the literature using MD simulations [27, 34, 35]. The sixteenth residues (Lysine, denoted as bold K in the amino acid sequences) along each peptide were modified from Lys to hydroxylysine (Hyl), which is an indispensable posttranslational modification for the formation of collagen fibrils [36]. This particular CMS (Fig. 1a) contains five negatively charged Asp and twelve positively charged residues including six Arg, three Hyl and three Lys. Thus, the CMS has a total charge of +7 e. Besides, the rest of the CMS is composed of a mixture of both polar (Q, N, H, S, T) and hydrophobic (A, I, L, M, F, P, G) residues. Based on the protonation state of amino acid side chains at neutral pH, Lys and Arg side chains were protonated while Asp chains were deprotonated. In this study, His were treated as neutral. We note that among all the types of residues presenting in natural collagens, only Val, Trp, Glu, hydroxyproline (Hyp) and Tyr are not included in this segment, among which Trp, Hyp and Tyr were reported to be strong binders of AuNS in the literature [14, 16, 17, 21, 31].

The utilized face-centred cubic [1 1 1] gold surface structure has a dimension of 137 Å × 139 Å × 12 Å (six-atoms thick). This structure allows the calculation of the full range of interactions with adsorbed atoms of the protein. The structure of the gold surface was generated from the Au (1 1 1) unit cell available in INTERFACE_FF_1_5 (https://bionanostructures.com/interface-md/), by utilizing the gmx nbox command in GROMACS 5.0.4 [37].

Molecular dynamics simulation protocol

To explore the molecular behaviour of proteins onto hydrophilic surfaces, MD simulations were performed on the adsorption of a CMS onto AuNS (denoted as Sys. 1). For comparison, MD simulations in explicit solvent were carried out to equilibrate the CMS under the absence of AuNS (denoted as Sys. 2), where no restraint was applied on the molecule. Detailed information of both systems about the water box type and dimension, counter ions type and number, number of gold atoms, as well as number of water molecules are showed in Table 1. In both systems, the solutes, i.e., the CMS and AuNS, were entirely solvated in an explicit TIP3P water box [38], making sure that the minimum distance between the biomolecule and the edge of water box is at least 10 Å. In total seven counter ions (Cl^-) were added to make the systems neutral, via tleap in AmberTools 16 [39]. In Sys. 1, the initial minimum distance between the CMS and AuNS is 12.5 Å, rendering the protein outside the cutoff range (within 10 Å) of the protein-AuNS dispersion interaction. To explore the adsorption mechanism of the CMS onto AuNS, in total 80 MD simulations were carried out for Sys. 1, where each simulation started from an identical CMS-AuNS complex conformation, without setting initial atomic velocities for the system. All MD simulations in the present study were carried out by the CUDA version of AMBER 16 biomolecular simulation package [40, 41] and the protein.ff14SB force field [42]. The force filed parameters for Hyl were taken from Ref. [43]. The interactions of solution with AuNS were described by the INTERFACE force field [44], where the equilibrium nonbonded distance r_0 is 2.951 Å, and the equilibrium nonbonded energy ε_0 is 5.29 kcal/mol [45]. This force field was previously used for investigating the adsorption of small peptides onto AuNS [32]. To avoid bad contacts within the systems, the geometry of the model was minimized using the following two processes. Firstly, the solutes were fixed by a harmonic potential of 50 kcal/mol·Å, while the water molecules were free to relax for 2000 steps, containing 1500 steepest decent steps followed by 500 conjugate gradient steps. Then, both the protein and solvent were free to relax for the same number of steepest decent and conjugate gradient steps. The geometrically minimized systems were heated from 0 K to 310K within 125 ps, where the protein were kept fixed by a positional restraint of 50 kcal/mol·Å. The heated systems were further equilibrated in an NPT ensemble for 500 ps at a constant pressure of one bar using the Berendsen barostat [46], during which process no restraint was applied on the collagen triple helix. Finally, the production run was carried out in an NPT ensemble. During this process, the temperature was kept at 310 K by the Langevin thermostat with gamma_ln set to 2 [47], and the pressure was held at one

bar using the Berendsen barostat [46] with a pressure coupling constant of 1 ps. In the present study, AuNS was treated as rigid, and therefore was kept fixed during the entire simulations for Sys. 1. The SHAKE algorithm was applied to restraint bond lengths involving hydrogens [48], which allows an integration time step of 2 fs. The particle mesh Ewald (PME) summation method was employed to calculate the long-range electrostatic interactions, where the cutoff distance for computing the non-bonded interaction is 10 Å. Periodic boundary conditions were used in all three dimensions. Model trajectories were saved every 2 ps for post data analysis. All of the 80 production runs on the Sys.1 were performed relatively long enough until the complex reaches the state where the N-terminal region (within five residues away from the cap Ace residues), the Middle region (residues from 12^{th} to 21^{st} along each chain) and the C-terminal region (within four residues away from the cap Nme residues) of the CMS have at least one residue adsorbed on AuNS. Apart from exploring the adsorption mechanism of proteins onto hydrophilic surfaces, we are interested in the structural change of collagen triple helices under the presence of AuNS. To this end, eight out of the total 80 production runs on the CMS-AuNS complex were carried out for 220 ns. For comparison, the production run of Sys. 2 with only the CMS was also performed for 220 ns.

Table 1. Model information of systems of the CMS in the presence and absence of AuNS.

Model information	Sys. 1	Sys. 2
Water box type	Triclinic	Octahedron
Water box dimension	157 Å × 159 Å × 90 Å	113 Å × 113 Å × 113 Å
Counter ions (number)	Cl^- (7)	Cl^- (7)
Number of gold atoms	8064	Nil
Number of water molecules	68651	33538

Data analysis were carried out in MATLAB 2016a [49], GROMACS 5.0.4 [37], and cpptraj in AmberTools 16 [39]. Visualization was done in UCSF Chimera 1.11.2 (http://www.cgl.ucsf.edu/chimera) [50] and plotting in GNUPLOT 4.6 (http://www.gnuplot.info).

Results

The present work explores the molecular behaviour of a human type I CMS under the presence of AuNS, via carrying out comprehensive MD simulations on the system of a CMS away from a planar gold surface. This aims to reveal the adsorption mechanism of proteins onto neutral hydrophilic surfaces at the atomic and molecular level.

Adsorption mechanism of the CMS onto AuNS

Protein-inorganic surface interactions are very common in nanotechnology and clinical applications. For example, it is inevitable for the metallic biomaterials implanted into the human body to interact with ECM proteins. Therefore, understanding the interaction of body proteins with inorganic surfaces such as titanium and stainless steels is crucial. This section explores the adsorption mechanism of proteins onto inorganic surface forming strong interactions with water.

In all of the 80 simulations, adsorption of the CMS onto AuNS adhered to the following three steps initially proposed for small peptides adsorption onto hydrophilic surfaces [32]: i) biased diffusion of the CMS from the bulk phase towards the water/AuNS interface; ii) anchoring of the CMS to the interface via forming hydrogen bonds with the interfacial layering water or direct hydrophobic interactions with the surface; iii) stepwise adsorption of the CMS onto AuNS and unfolding of the CMS, where the protein groups gradually displace the water immediately above AuNS in a sequential fashion and rearrange themselves to maximize the interaction with AuNS. For further explanation, here we consider an exemplar trajectory showed in Fig. 1.

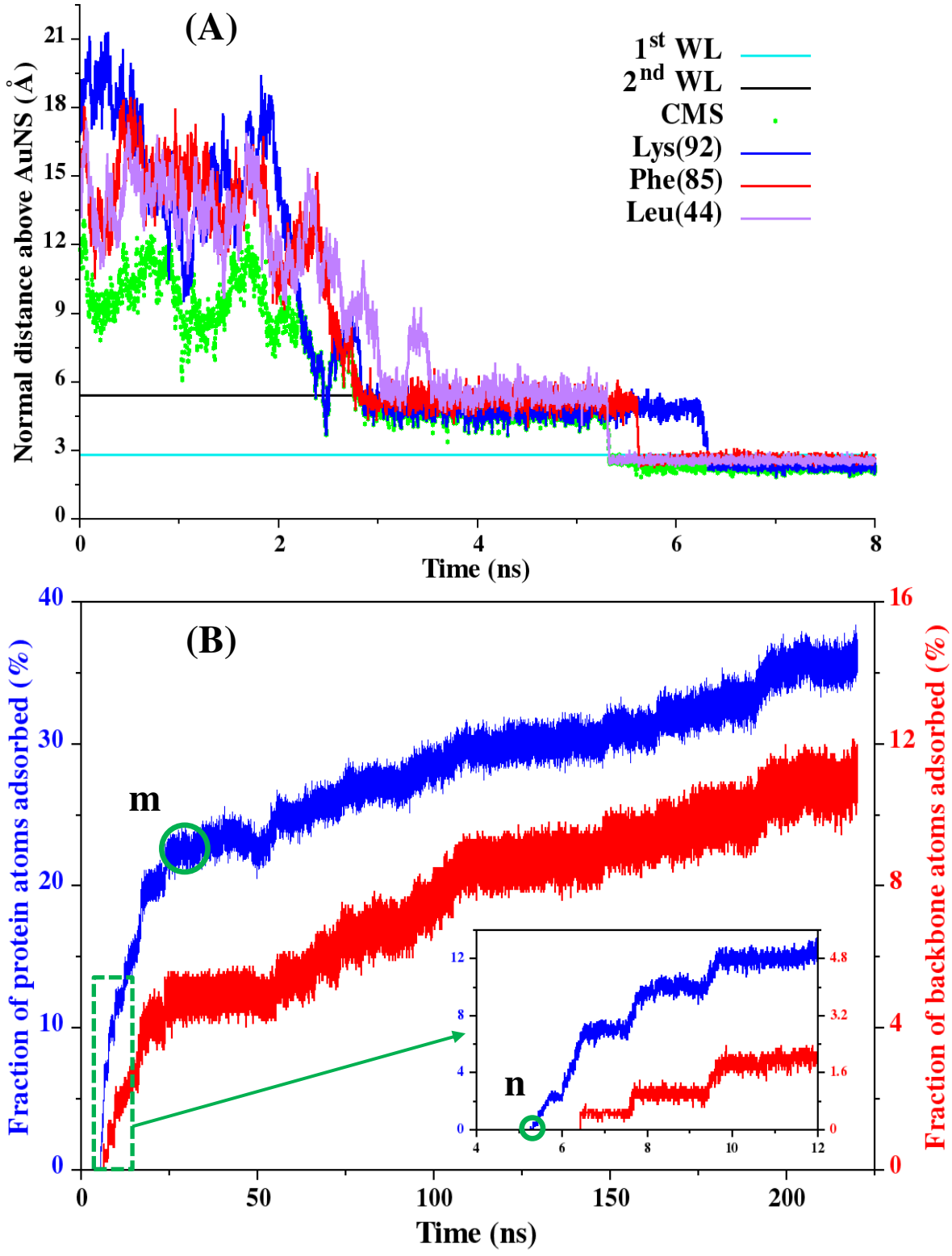
(A)
1st WL
2nd WL
CMS
Lys(92)
Phe(85)
Leu(44)
Normal distance above AuNS (Å)
Time (ns)
(B)
m
n
Fraction of protein atoms adsorbed (%)
Fraction of backbone atoms adsorbed (%)
Time (ns)

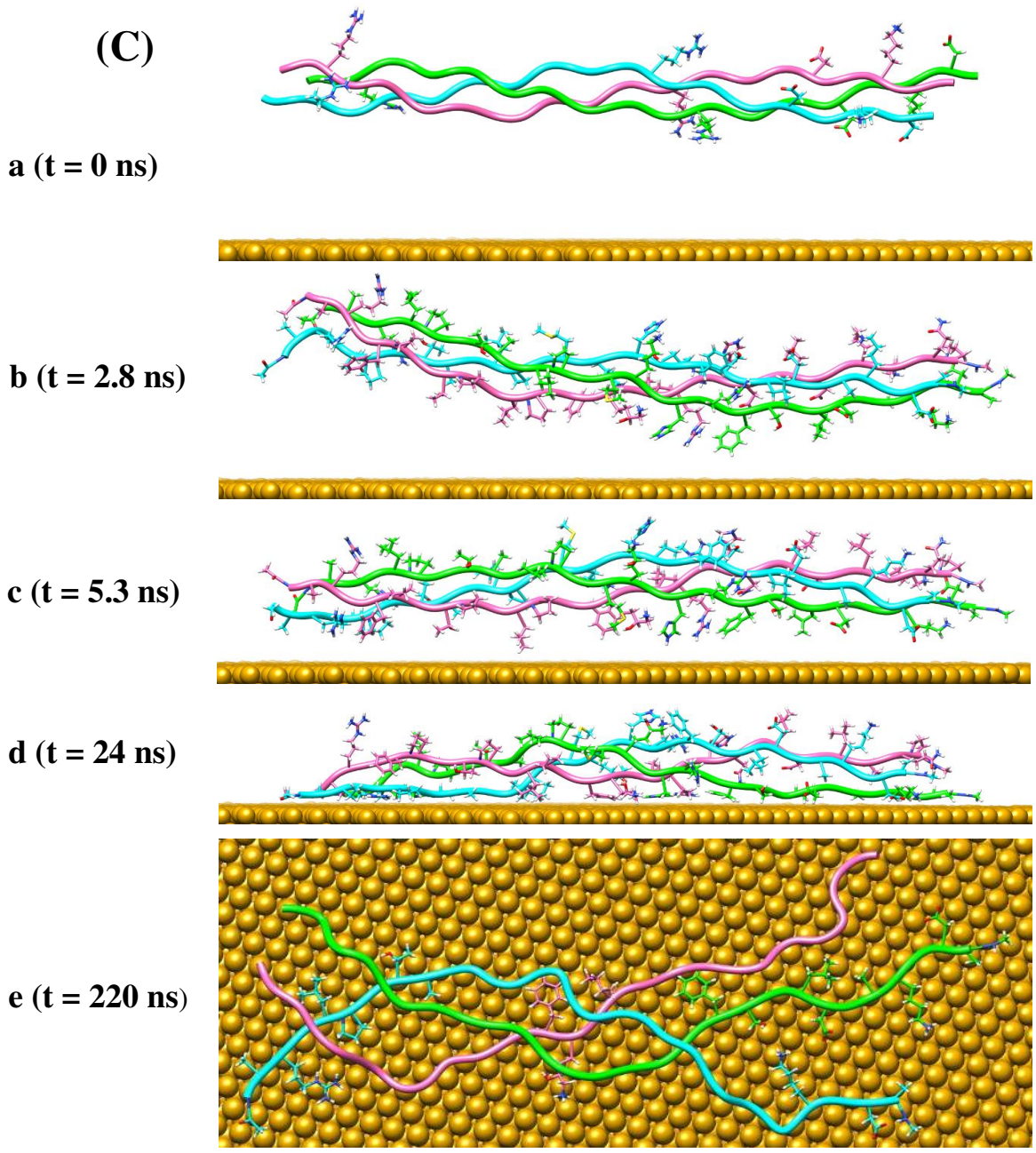

Fig. 1 An exemplar trajectory of the MD simulations on the CMS-AuNS complex: (A) from the start up to somewhere beyond the initiation of adsorption, the variation of the minimum normal distance above AuNS of the CMS (green dot) and three representative residues in this simulation. Here, the two horizontal lines denote positions of the first water layer (cyan) and the second water layer (black) above AuNS; (B) evolution of the fraction of the number of adsorbed protein atoms (blue) and backbone atoms (red), where: c suggests the initiation of protein adsorption, and d indicates that adsorption and unfolding of the CMS starts to occur at a much slower rate. Atoms within 3.5 Å of AuNS were considered as adsorbed on the surface. The fraction of adsorbed backbone atoms increased in a consistent stepwise pattern with that of the increase of the total adsorbed protein atoms, indicating that adsorption and unfolding of the CMS occur simultaneously; (C) representative snapshots of the CMS-AuNS complex reflecting the stepwise adsorption

process: a initial conformation of the complex, where only side chains of charged residues are displayed; b conformation of the complex at the initiation of anchoring; c conformation of the complex at the initiation of adsorption; d conformation of the complex when adsorption and unfolding of the CMS started to occur at a much slower rate; e final snapshot of the complex in this simulation.

Biased diffusion

Despite starting from an identical initial conformation of the CMS-AuNS complex, the trajectories of the CMS in all the simulations for Sys. 1 diverged rapidly. This indicates that the protein was still in a diffusional state at the beginning of the simulations. Fig. 1(A) demonstrates that the protein diffused from the bulk phase towards AuNS, even though the groups closest to AuNS initially were outside the cutoff range of the dispersion interaction explicitly considered between the protein and AuNS, i.e., the protein was initially beyond 10 Å away from the surface. Similar behaviour was observed for the CMS in other simulations undertaken on the CMS-AuNS complex. This is consistent with the work by Penna et al. [32], where the A3 peptide and the SD125 peptide were found to diffuse towards the gold surface and the platinum surface in all of the 84 and 165 MD simulations, respectively. In this work, Penna and co-authors revealed that the biased diffusion is induced by a long-range force existing between the biomolecule and AuNS [32]. For detailed information on the underlying mechanism of the biased diffusion, we recommend referring to the literature [32].

Anchoring

The anchoring phase refers to the process whereby the protein engages with the interfacial layering water and steps into the 2nd water layer adjacent to AuNS. Despite the identical initial conformation of the CMS-AuNS complex, the first anchoring pattern of the CMS with AuNS was formed through different anchoring residues after different simulation time, due to the diffusional nature of the CMS at the beginning of the simulations. This behaviour is in accordance with work by Hoefling and co-workers [14, 15, 28] and Penna et al. [32], where AuNS was reported to only form strong interactions with single amino acids and peptides located within 8 Å away from the gold surface. Identical to the work by Penna [32], the anchoring process of the CMS to AuNS is reversible, as reflected in the exemplar trajectory of Fig. 1(A).

Among the residues involved in the first anchoring events occurring in all of the 80 simulations, there are 28 located in the N-terminal region, 4 in the Middle region and 48 in the C-terminal

region. The remarkable difference in the rate between the N-terminal region and the C-terminal region that initiated the first anchoring process of the protein originates from the non-uniform charge distribution of the CMS (Fig. 1a) and the charged layers adjacent to the gold surface [32]. Besides, residues in the Middle region initiating the first anchoring event only occurred in 5% of all the simulations, despite the existence of many polar residues with long side chains in the Middle region. This is due to the fact that the length (~ 92 Å) of the CMS studied here is shorter than the persistence length (~ 145 Å) of the type I collagen molecule [51]. On the other hand, collagen molecule peptides with similar lengths appear to be slightly bent in water [52], thus rendering residues in the Middle region with long side chain capable of engaging the protein with the gold surface. In summary, the initial anchoring pattern of the protein to AuNS is intimately related to the protein structure and the chemical nature of the constituent residues.

Fig. 2 displays the proportion of the anchoring events initiated by different residues, where the three parts from left to right correspond to those in the N-terminal region, the Middle region and the C-terminal region, respectively. Consistent with the work by Penna et al. [32], hydrophilic groups of the CMS and their interactions with the interfacial water molecules play an important role in the anchoring events (Fig. 2). Notably, Lys(92), which is four residues away from the cap residue Nme(96), initiated 38.5% of the entire 109 anchoring events alone, where around half of the time it was accompanied by Asp (30) via forming hydrogen bond between side chains. Compared to Lys92, Lys 60 showed a much lower propensity of anchoring. This stems from the CMS structure and its initial relative position to AuNS: i) three polypeptides intertwine with one residue shifted to the other, thus making Lys(92) positioned in a more flexible region than Lys(60); ii) Lys(92) often forms hydrogen bond with Asp(30), resulting in a group with higher anchoring propensity to AuNS; iii) in the starting conformation of the complex, the side chain of Lys(92) points towards AuNS, whereas the side chain of Lys(60) faces upwards, thus allowing Lys(92) higher chance to diffuse more quickly to AuNS than Lys60. In addition, Fig. 2 suggests that 20.2% of the anchoring events were initiated by the cap residues, where Ace(1) initiated 40.5% of the anchoring events involving the N-terminal region while only 11% of the anchoring events involving the C-terminal region was triggered by Nme(96). The remarkable difference in the anchoring propensity between Ace(1) and Nme(96) may originate from: i) Ace(1) is connected by Gly(2), while Nme(96) is connected to Ala(95), making Ace(1) more flexible than Nme(96); ii) charged Lys(92) with long

side chain forms hydrogen bond with Asp(30), thus forming a group with a much higher anchoring propensity. Interestingly, initiation of the total 109 anchoring events only involved the N-terminal cap of chain A (Ace(1)), and the C-terminal cap of chain C (Nme(96)). A closer look at the triple helical structure reveals that the other four cap residues all form hydrogen bonds with neighbouring polypeptides, which confines their flexibility thus reducing their propensity to engage with the interfacial water. Above all, our results reveal that the anchoring propensity of a protein residue are closely related to the protein structure, as well as the chemical nature of the residue and its neighbouring residues.

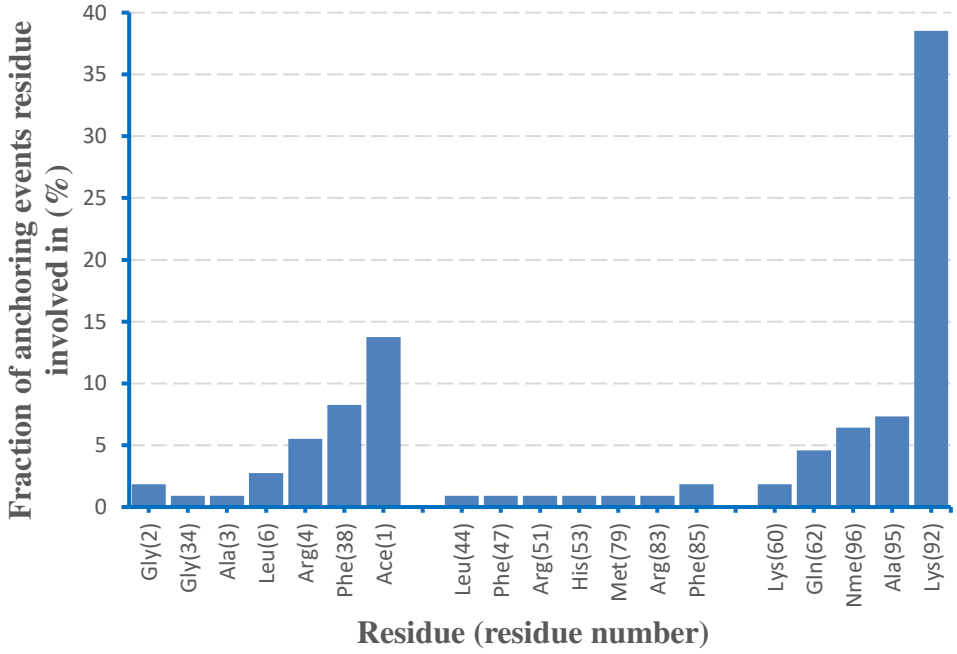

Fig. 2 Fraction of anchoring events activated by different residues. An anchoring event is counted when the CMS starts to engage with the water/surface via an amino acid which remains around the second water layer for a certain amount of time (usually ranging from 0.5 ns to couple of nanoseconds). The total number of anchoring events observed in the 80 simulations is 109. The fraction of anchoring events activated by a certain residue is calculated as the number of anchoring events activated by this residue divided by the total number of anchoring events.

Stepwise adsorption

The adsorption phase is defined as the process where the anchored protein gradually rearranges itself to displace the 1st interfacial water molecules, thus forming direct contact with the surface. The anchored protein needs to adjust itself and then wait until it is able to insert its groups into the 1st tightly bound water layer above AuNS. Consequently, the adsorption process of the protein is always slow and stepwise as indicated in the exemplar trajectory of Fig. 1(B). Data analysis

revealed that hydrophilic groups show higher propensity to activate adsorption of the molecule onto AuNS (Fig. S1), which is consistent with the work reported by Penna and co-authors [32].

We are also interested in investigating the factors that determine which group to be the second and subsequent to adsorb onto the surface. While hydrophilic residues present much higher propensity to initiate adsorption, Penna and co-authors [32] found that the probability of a peptide group being the second and subsequent to adsorb is exponentially related to their distance from the initial adsorbed group and the groups already adsorbed respectively, rather than depending on the chemical nature of the group. Interestingly, the present study clearly suggests a different case. Here, we give another exemplar trajectory performed on the CMS-AuNS complex as displayed in Fig. 3(A). In the case of this trajectory, Ala(3) close to the N-termini initiated adsorption of the CMS to AuNS, followed by subsequent adsorption of the cap residue Ace(1) and the neighbouring Gly(2). However, Ala(95), which is close to the C-termini, presented to be the fourth residue to pop into the 1st interfacial water layer, thus leading to an arch-like conformation of the CMS as displayed in Fig. 3(B). Similar conformation was observed for a collagen-like peptide by Gopalakrishnan and co-workers [27], where only two terminal regions adsorbed onto the gold surface throughout their entire simulation. The arch-like conformation of the CMS in Fig. 3(B) is dictated by the preferred slight bending configuration of the CMS in water [52]. In summary, our results demonstrate that apart from the distance from the initial adsorbed group and the groups already adsorbed, the protein group being the second and subsequent to adsorb is also related to the initial contact pattern of the protein-surface complex and the structural properties of the protein such as the flexibility.

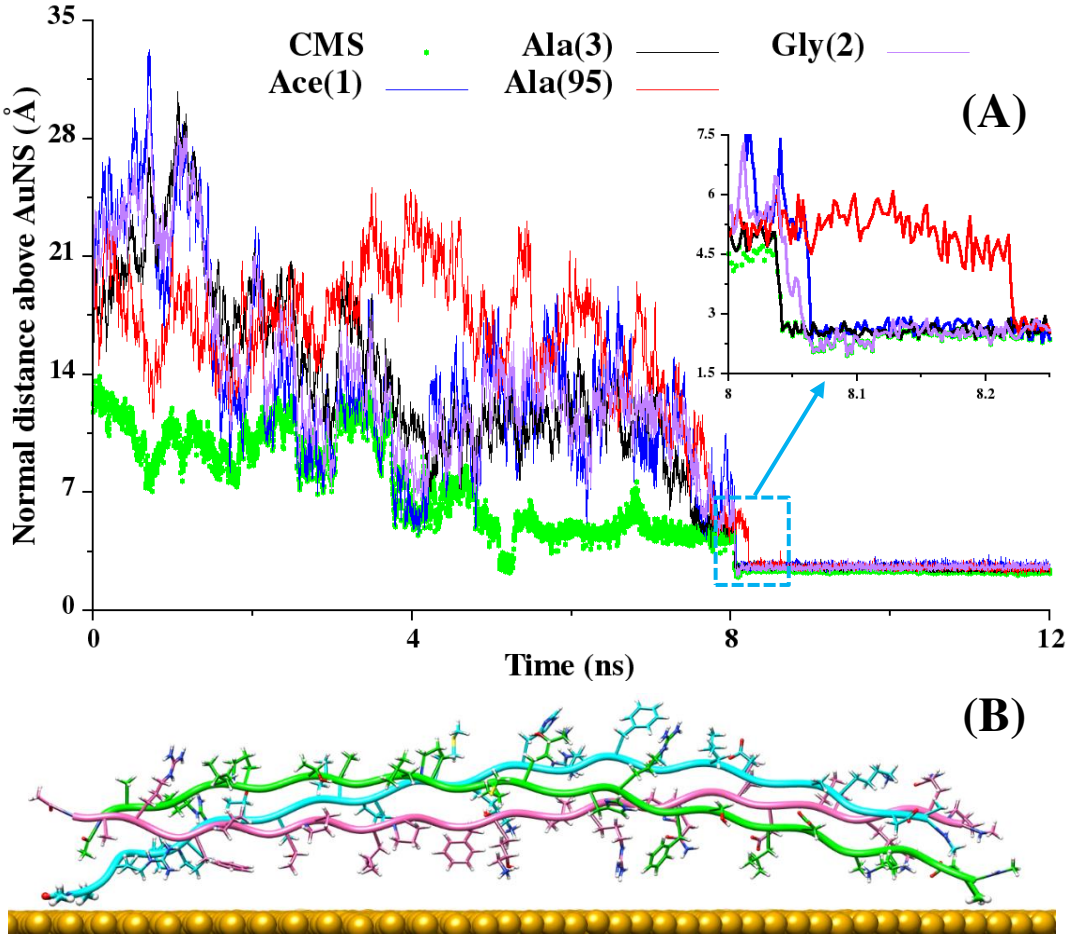

Fig. 3 (A) An exemplar trajectory of the MD simulations on the CMS-AuNS complex: from the start up to somewhere beyond the initiation of adsorption, the variation of the minimum normal distance above AuNS of the CMS and the first four residues adsorbing onto the surface in this simulation; (B) a snapshot of the CMS-AuNS complex, corresponding to adsorption initiation of the Ala(95) which is the fourth residue to adsorb on the surface.

It is of great significance to reveal whether the protein desorbs after forming direct contact with the gold surface. Previous MD simulations regarding proteins adsorption onto AuNS demonstrated that proteins do not desorb from the surface after the initiation of adsorption [28, 29]. Interestingly, our results clearly show that the adsorption process is not always irreversible: the CMS in twelve of the total 80 simulations desorbed sometime after it formed direct contact with AuNS. For example, in the exemplar trajectory of Fig. 3(A), the protein desorbed ~178 ps after Arg(18) triggered its adsorption onto AuNS. The small desorption fraction observed here may be related to the previously reported low desorption rate of various peptides onto metal surfaces including AuNS [53], as well as the reversible association of the GB3 protein with the gold nanoparticle [54]. Detailed information of the adsorption events regarding the initiating residue, starting time, and

duration in the twelve cases are displayed in Table 2. As illustrated in Table 2, the protein can desorb from AuNS after adsorbing for more than 1 ns. We note that the residues initiating both adsorption events are not necessarily to be the same, and can be located in different regions of the protein. Notably, residues that triggered adsorption of the protein and then desorbed away from the surface are all positively charged residues with long side chains, including ten Lys(92), one Hyl(80) and one Arg(68). Similarly, Lys residues partially detached from the Au (1 1 1) surface as well as the Pd-Au (1 1 1) bimetal surface was reported in an MD simulation study [18]. Besides, charged termini of the SD152 and A3 peptides presented prominent 'dynamic' lockdown behaviour onto the solid surfaces strongly interacting with water, where they repeatedly popped in and out of the 1st interfacial water layer [32]. The quick desorbing phenomenon observed for the SD152 and A3 peptides [32] may be because they lack positively charged Arg and Lys. The origin of the desorption behaviour of Lys remains not fully understood, although the binding affinity of Lys to AuNS is small as revealed in experiments conducted by Willett et al. [55]. However, the reversible adsorption behaviour may originate from thermal fluctuations repeatedly taking the positively charged residues into the disfavoured like-charge region between the water layers [32], from which they are ejected soon after back into more favoured negatively charged water layers. Closer analyses of the trajectories suggest that in the duration of the 1st adsorption events, side chains of those positively charged residues remain pointing towards the surface, as displayed in Fig. 4. In simulations performed on the complex, some other residues also presented desorption behaviour after their side chains adsorbed on the surface for a certain time so as to adjust the protein conformation for a more stable structure. However, no residue was observed to desorb from AuNS once its backbone atoms interact with the surface.

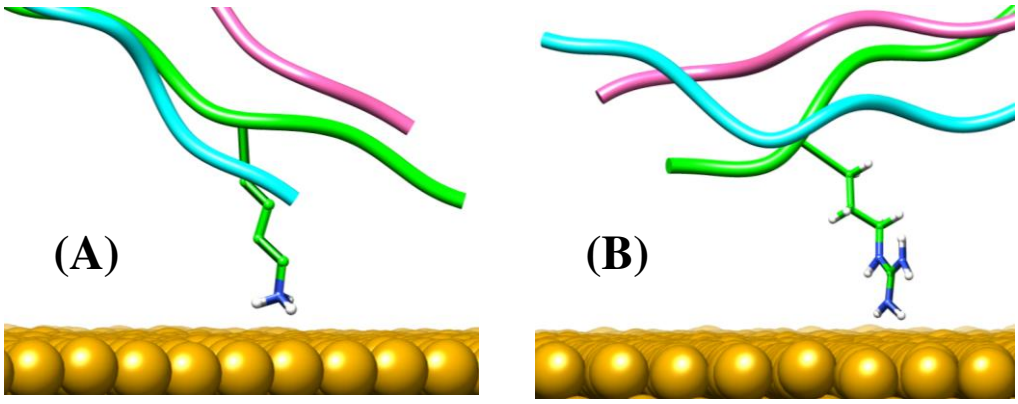

Fig. 4 Representative conformation of (A) Lys and (B) Arg in the first adsorption event of an exemplar trajectory evolving reversible adsorption of the CMS.

Table 2. Information of the first and second adsorption events observed in the twelve trajectories involving reversible adsorption.

Case	First adsorption event			Second adsorption event	
	Initiating residue	Starting time (ns)	Duration (ps)	Initiating residue	Starting time (ns)
1	Lys(92)	1.038	42	His(82)	5.276
2	Lys(92)	6.212	54	Nme(96)	6.424
3	Lys(92)	4.320	80	Lys(92)	4.760
4	Lys(92)	1.906	94	Asp(30)	4.950
5	Hyl(80)	2.620	140	Arg(4)	3.012
6	Arg(68)	5.094	178	Ala(3)	8.042
7	Lys(92)	3.588	506	Lys(92)	4.852
8	Lys(92)	3.860	518	Nme(96)	4.872
9	Lys(92)	4.590	588	Lys(92)	5.388
10	Lys(92)	2.054	610	Lys(92)	2.896
11	Lys(92)	8.844	1140	Gln(62)	10.516
12	Lys(92)	1.850	1342	Lys(92)	3.826

In summary, all of the MD simulations on the CMS-AuNS complex performed in this work adhered to the three-step adsorption process (i.e., biased diffusion, anchoring and stepwise adsorption), which was previously proposed for the adsorption of small peptides onto hydrophilic solid surfaces [32]. The obtained three-step adsorption mechanism of proteins onto AuNS can be extended to other types of hydrophilic surfaces with charged layers originating from the orientational structuring of the interfacial layering water. However, the adsorbed configuration of a certain protein may vary among different hydrophilic surfaces, due to their different binding modes. For example, MD simulations yielded flatter conformations on Au and a greater variety of three dimensional adsorbed configurations on Ag, indicating enthalpically driven binding on Au and entropically driven binding on Ag[26].

This study provides significant insights into biomedical applications. Firstly, the biased diffusion induced rapid association of the collagen-AuNS complex indicates that no bare AuNPs exist in the ECM. Therefore, the bioactivity of bare AuNPs is closely related to its administration history and the proteins present during the initial association of the protein with AuNPs. In addtion, different

contact patterns of the CMS-AuNS complex and the fast adsorption of the CMS onto AuNS observed here reveal the rather unspecific binding nature of bare AuNPs, which indicates the potential health risks of bare AuNPs for biomedical applications.

Conformational changes of the CMS on AuNS

Interestingly, the CMS in all 8 production runs that were extended to 220 ns unfolded severely on AuNS. Detailed atomic-level analysis revealed that this unfolding originates from the direct interactions between the CMS backbone and the gold surface [56].

In contrast to unfolding under the presence of AuNS, visualization of the trajectory from the simulation of Sys. 2 suggests that the CMS preserved its secondary structure under the absence of AuNS during the simulation. To further probe the effect of AuNS on the structure of the CMS, we investigated the conformational changes of the CMS along the simulation time, both in the presence (exemplar trajectory of Fig. 1) and in the absence of AuNS. The conformational changes are characterized by the variation of number of inter-chain hydrogen bonds and geometric parameters including the average radius of the triple helix and Ramachandran angles of the comprising residues. Our analysis clearly shows that the Au (1 1 1) surface interacts with the CMS, which confines the formation of the inter-chain hydrogen bond, thus leading to a significant unfolding of the collagen triple-helical structure. This readily, severe unfolding phenomenon suggests the potential health risks of bare AuNPs for therapeutic and biomedical applications.

Inter-chain hydrogen bonds

The triple-helical structure of collagen molecules is stabilized by the conventional inter-chain hydrogen bonds. Hence, to further investigate the structural stability of the CMS in the presence of AuNS, we monitored the variation of number of inter-chain hydrogen bonds with respect to time as presented in Fig. 5(A). In this study, the presence of hydrogen bonds were analysed according to the geometric criteria: a distance of less than 3 Å between donor and acceptor, and a donor nitrogen, donor hydrogen and acceptor oxygen bond angle greater than 120°. The number of inter-chain hydrogen bonds of the CMS in Sys. 2 remained stable at an average number of 30 during the whole production run (green data points in Fig. 5(A)), as there exists one inter-chain hydrogen bond per triplet [57]. Consequently, the triple-helical structure of the CMS was entirely preserved in the absence of AuNS. In contrast, the occupancy of inter-chain hydrogen bonds of

the CMS in the presence of AuNS decreased drastically in a stepwise pattern (blue data points in Fig. 5(A)). Initially, the number of inter-chain hydrogen bonds in Sys 1 were stable at ~30 within 7.5 ns, indicating an intact triple-helical structure of the CMS. This is consistent with the evolution of the trajectory as described in Fig. 1(A). Then, the number of inter-chain hydrogen bonds started to decline stepwise to an average number of seven at the end of the simulation. The remarkable decrease in the number of inter-chain hydrogen bonds of the CMS clearly indicates a severe unfolding of the triple helix in the presence of AuNS, which is in accordance with the final configuration of the CMS-AuNS complex displayed in Fig. 1e. The variation in the number of inter-chain hydrogen bonds obtained from both systems is comparable with the evolution of the diameter and other geometric parameters discussed in the following sections.

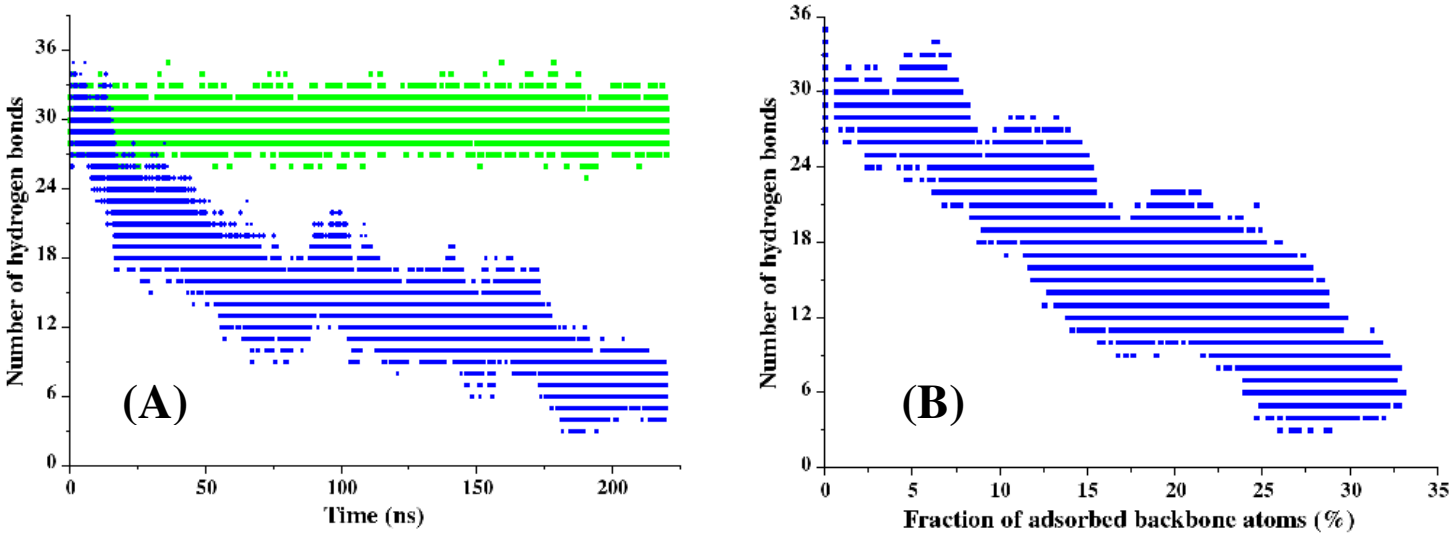

Fig. 5 Variation of number of inter-chain hydrogen bonds of the CMS (A) with respect to time in the presence (blue) and absence (green) of AuNS, (B) with respect to the fraction of the number of adsorbed backbone atoms to the total number of the backbone atoms of the CMS.

It is also interesting to examine the variation of number of inter-chain hydrogen bonds of the CMS with respect to the number of interactions between the CMS and AuNS. Fig. 5(B) shows the variation of the number of inter-chain hydrogen bonds of the CMS as a function of the fraction of the number of adsorbed backbone atoms to the total number of the protein backbone atoms. As illustrated in Fig. 5(B), before adsorption onto AuNS, the number of inter-chain hydrogen bonds remained stable at ~30. Upon adsorption onto AuNS, the number of inter-chain hydrogen bonds presented a stepwise decrease. This stepwise drop in the number of inter-chain hydrogen bonds originates from the stepwise adsorption of the CMS on AuNS. This reflects that the CMS interacts

with AuNS via its backbone after adsorbing on AuNS, thus confining the formation of the inter-chain hydrogen bonds.

Diameter of the triple helix

Normal collagen molecules in nature adopt a diameter of approximately 1.5 nm. The unfolding probability of collagen molecules is indicated in the diameter (D) of the triple helix as reported in a previous study [58]. To further quantify the unfolding of the CMS in the presence of AuNS, time evolution of the average diameter of the triple helix in both systems were calculated via MATLAB and displayed in Fig. 6. The diameter of the CMS was averaged from diameters of the circles encompassed by each set of the three Cα-atoms in the three peptides forming the triple helix, while the schematic representation of the description of diameter is demonstrated in the literature [27]. As seen from Fig. 6, the average radius of the CMS in the absence of AuNS remained stable at ~0.87 nm, while the average diameter of the CMS in the presence of AuNS increased during the production run. At the beginning of the simulation (within ~7.5 ns), the average radius of the triple helix in the presence of AuNS were stable at approximately 0.87 nm, reflecting the structural intact of the triple helix. Then, the average radius of the triple helix increased significantly to ~1.5 nm at the end of the simulations, indicating a severe unfolding of the triple-helical structure.

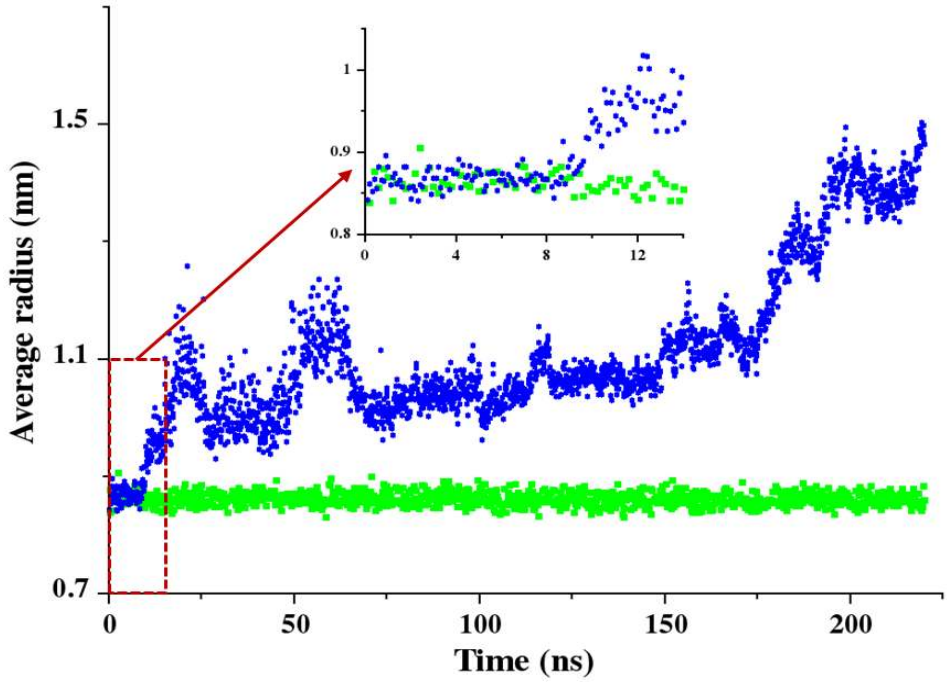

Fig. 6 Time evolutions of average radius of the CMS in the presence (blue) and absence (green) of AuNS.

Ramachandran angles

Collagen molecule polypeptides carry a polyproline II secondary structure, where sequential residues all adopt (φ, ψ) backbone dihedral angles of roughly (-75°, 150°). For collagen molecule triple helices, (φ, ψ) is slightly different among different residues, depending on the position of the residue in the Gly-X-Y triplet and whether the triplet contains imino residues (i.e., Pro or Hyp). For detailed information on the exact values of the Gly, X and Y residues in the triplets with and without imino residues, we recommend referring to Ref. [59]. The polyproline II secondary structure of the three chains are essential for the formation of the collagen molecule triple helix. Hence, information of the Ramachandran angles of the constituent residues contributes to a better understanding of the triple-helical conformation of the CMS. Fig. 7 shows the Ramachandran angles (φ, ψ) for all residues of the CMS calculated from both systems. In Fig. 7, the Ramachandran angles for the CMS in Sys. 2 were averaged from the trajectories of the final 100 ns production run, whereas the Ramachandran angles for the CMS in Sys. 1 were directly computed from the CMS structure in the final frame of the simulation. As we can see from Fig. 7, the Ramachandran angles of the residues in the CMS in Sys. 2 mostly remained in the polyproline II region of the Ramachandran plot, except those of the terminal residues. On the contrary, most of the Ramachandran angles of the residues in the CMS under the presence of AuNS deviated from the values indispensable for the formation of the collagen triple helix in terms of the Ramachandran angles, which indicates the loss of the polyproline II secondary structure of the ploypeptides thus inducing a remarkable unfolding of the protein in the presence of AuNS.

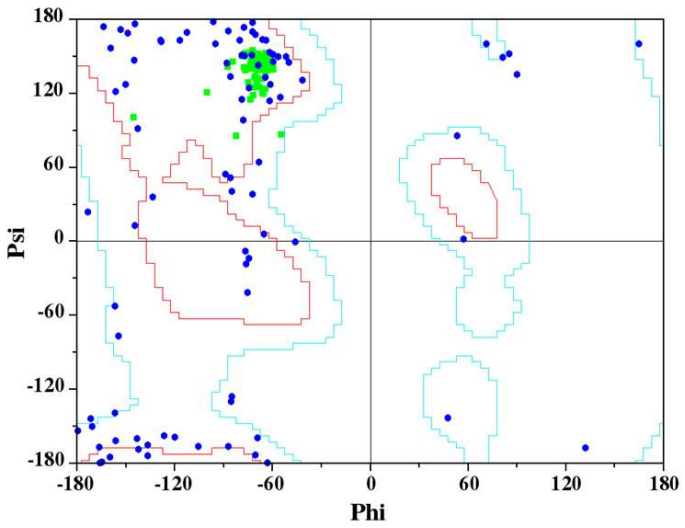

Fig. 7 Ramachandran angles for residues of the CMS in the presence (blue) and absence (green) of AuNS. The red (turquoise) region indicates the favored (allowed) region defined by ProCheck.

Conclusions

By interrogating the results of comprehensive MD simulations on the CMS-AuNS complex, we find that the stepwise adsorption mechanism (i.e., biased diffusion, anchoring and stepwise adsorption) obtained for proteins onto hydrophilic surfaces is identical to that previously proposed for small peptides [32]. This is because the adsorption mechanism of biomolecules onto hydrophilic surfaces is dictated by the existence of the charged layers above the surface, due to the interfacial water layers and the orientational ordering of the interfacial layering water molecules [32]. However, some of the adsorption behaviors of the CMS onto AuNS differ from those previously reported for small peptides [32], due to the cooperative behaviors of proteins adsorption onto solid surfaces. The obtained adsorption mechanism of proteins onto hydrophilic surfaces may shed light on the development and manufacture of inorganic surfaces, for example, AuNPs and metallic implant biomaterials, for biomedical and clinical applications. In addition, collagen triple helices presented to unfold readily on gold surfaces. This unfolding phenomenon advices the potential health risks of bare AuNPs for biomedical and therapeutic applications.

Conflicts of interest

The authors declare that they have no conflict of interest.

Acknowledgements

The authors thank Hendrik Heinz (Department of Chemical and Biological Engineering, University of Colorado at Boulder, Boulder, Colorado, USA) for his detailed explanations of the INTERFACE force field. This research was funded by ARC Discovery project (DP150100828). The High Performance Computing resources provided by Queensland University of Technology (QUT) are gratefully acknowledged. Also, the financial support of China Scholarship Council (CSC) scholarship from Chinese government and Top-up scholarship from QUT are greatly appreciated.

Supporting Information

Fraction of adsorption initiated by different residues

References

1. Demann, E. T.; Stein, P. S.; Haubenreich, J. E., Gold as an implant in medicine and dentistry. *Journal of Long-term Effects of Medical Implants* **2005,** *15* (6), 687-698.
2. Auffan, M.; Rose, J.; Bottero, J.-Y.; Lowry, G. V.; Jolivet, J.-P.; Wiesner, M. R., Towards a definition of inorganic nanoparticles from an environmental, health and safety perspective. *Nature Nanotechnology* **2009,** *4* (10), 634-641.
3. Matsuno, H.; Yokoyama, A.; Watari, F.; Uo, M.; Kawasaki, T., Biocompatibility and osteogenesis of refractory metal implants, titanium, hafnium, niobium, tantalum and rhenium. *Biomaterials* **2001,** *22* (11), 1253-1262.
4. Ozboyaci, M.; Kokh, D. B.; Corni, S.; Wade, R. C., Modeling and simulation of protein–surface interactions: achievements and challenges. *Quarterly Reviews of Biophysics* **2016,** *49*, 1-45.
5. Alava, T.; Mann, J. A.; Théodore, C. c.; Benitez, J. J.; Dichtel, W. R.; Parpia, J. M.; Craighead, H. G., Control of the graphene–protein interface is required to preserve adsorbed protein function. *Analytical Chemistry* **2013,** *85* (5), 2754-2759.
6. Sun, J.; Xianyu, Y.; Jiang, X., Point-of-care biochemical assays using gold nanoparticle-implemented microfluidics. *Chemical Society Reviews* **2014,** *43* (17), 6239-6253.
7. Lei, Y.; Tang, L.; Xie, Y.; Xianyu, Y.; Zhang, L.; Wang, P.; Hamada, Y.; Jiang, K.; Zheng, W.; Jiang, X., Gold nanoclusters-assisted delivery of NGF siRNA for effective treatment of pancreatic cancer. *Nature Communications* **2017,** *8*, 15130.
8. Giacomelli, C. E.; Norde, W., The adsorption–desorption cycle. Reversibility of the BSA–silica system. *Journal of Colloid and Interface Science* **2001,** *233* (2), 234-240.
9. Long, J. R.; Shaw, W. J.; Stayton, P. S.; Drobny, G. P., Structure and dynamics of hydrated statherin on hydroxyapatite as determined by solid-state NMR. *Biochemistry* **2001,** *40* (51), 15451-15455.
10. Kim, D. T.; Blanch, H. W.; Radke, C. J., Direct imaging of lysozyme adsorption onto mica by atomic force microscopy. *Langmuir* **2002,** *18* (15), 5841-5850.
11. Johnson, C.; Yuan, Y.; Lenhoff, A., Adsorbed layers of ferritin at solid and fluid interfaces studied by atomic force microscopy. *Journal of Colloid and Interface Science* **2000,** *223* (2), 261-272.
12. Cohavi, O.; Corni, S.; De Rienzo, F.; Di Felice, R.; Gottschalk, K. E.; Hoefling, M.; Kokh, D.; Molinari, E.; Schreiber, G.; Vaskevich, A., Protein–surface interactions: challenging experiments and computations. *Journal of Molecular Recognition* **2010,** *23* (3), 259-262.
13. Charchar, P.; Christofferson, A. J.; Todorova, N.; Yarovsky, I., Understanding and Designing the Gold–Bio Interface: Insights from Simulations. *Small* **2016,** *12* (18), 2395-2418.
14. Hoefling, M.; Iori, F.; Corni, S.; Gottschalk, K.-E., Interaction of amino acids with the Au (111) surface: adsorption free energies from molecular dynamics simulations. *Langmuir* **2010,** *26* (11), 8347-8351.
15. Hoefling, M.; Iori, F.; Corni, S.; Gottschalk, K. E., The conformations of amino acids on a gold (111) surface. *ChemPhysChem* **2010,** *11* (8), 1763-1767.
16. Wright, L. B.; Rodger, P. M.; Corni, S.; Walsh, T. R., GolP-CHARMM: first-principles based force fields for the interaction of proteins with Au (111) and Au (100). *Journal of Chemical Theory and Computation* **2013,** *9* (3), 1616-1630.
17. Feng, J.; Pandey, R. B.; Berry, R. J.; Farmer, B. L.; Naik, R. R.; Heinz, H., Adsorption mechanism of single amino acid and surfactant molecules to Au {111} surfaces in aqueous solution: design rules for metal-binding molecules. *Soft Matter* **2011,** *7* (5), 2113-2120.
18. Heinz, H.; Farmer, B. L.; Pandey, R. B.; Slocik, J. M.; Patnaik, S. S.; Pachter, R.; Naik, R. R., Nature of molecular interactions of peptides with gold, palladium, and Pd− Au bimetal surfaces in aqueous solution. *Journal of the American Chemical Society* **2009,** *131* (28), 9704-9714.

19. Yu, J.; Becker, M. L.; Carri, G. A., The influence of amino acid sequence and functionality on the binding process of peptides onto gold surfaces. *Langmuir* **2011,** *28* (2), 1408-1417.
20. Hughes, Z. E.; Kochandra, R.; Walsh, T. R., Facet-Specific Adsorption of Tripeptides at Aqueous Au Interfaces: Open Questions in Reconciling Experiment and Simulation. *Langmuir* **2017,** *33* (15), 3742-3754.
21. Tang, Z.; Palafox-Hernandez, J. P.; Law, W.-C.; E. Hughes, Z.; Swihart, M. T.; Prasad, P. N.; Knecht, M. R.; Walsh, T. R., Biomolecular recognition principles for bionanocombinatorics: an integrated approach to elucidate enthalpic and entropic factors. *ACS Nano* **2013,** *7* (11), 9632-9646.
22. Feng, J.; Slocik, J. M.; Sarikaya, M.; Naik, R. R.; Farmer, B. L.; Heinz, H., Influence of the shape of nanostructured metal surfaces on adsorption of single peptide molecules in aqueous solution. *Small* **2012,** *8* (7), 1049-1059.
23. Verde, A. V.; Acres, J. M.; Maranas, J. K., Investigating the specificity of peptide adsorption on gold using molecular dynamics simulations. *Biomacromolecules* **2009,** *10* (8), 2118-2128.
24. Heinz, H., Computational screening of biomolecular adsorption and self‐assembly on nanoscale surfaces. *Journal of Computational Chemistry* **2010,** *31* (7), 1564-1568.
25. Vila Verde, A.; Beltramo, P. J.; Maranas, J. K., Adsorption of homopolypeptides on gold investigated using atomistic molecular dynamics. *Langmuir* **2011,** *27* (10), 5918-5926.
26. Palafox-Hernandez, J. P.; Tang, Z.; Hughes, Z. E.; Li, Y.; Swihart, M. T.; Prasad, P. N.; Walsh, T. R.; Knecht, M. R., Comparative study of materials-binding peptide interactions with gold and silver surfaces and nanostructures: a thermodynamic basis for biological selectivity of inorganic materials. *Chemistry of Materials* **2014,** *26* (17), 4960-4969.
27. Gopalakrishnan, R.; Singam, E. A.; Sundar, J. V.; Subramanian, V., Interaction of collagen like peptides with gold nanosurfaces: a molecular dynamics investigation. *Physical Chemistry Chemical Physics* **2015,** *17* (7), 5172-5186.
28. Hoefling, M.; Monti, S.; Corni, S.; Gottschalk, K. E., Interaction of β-sheet folds with a gold surface. *PloS One* **2011,** *6* (6), e20925.
29. Ozboyaci, M.; Kokh, D.; Wade, R., Three steps to gold: mechanism of protein adsorption revealed by Brownian and molecular dynamics simulations. *Physical Chemistry Chemical Physics* **2016,** *18* (15), 10191-10200.
30. Corni, S.; Hnilova, M.; Tamerler, C.; Sarikaya, M., Conformational Behavior of Genetically-Engineered Dodecapeptides as a Determinant of Binding Affinity for Gold. *The Journal of Physical Chemistry C* **2013,** *117* (33), 16990-17003.
31. Hnilova, M.; Oren, E. E.; Seker, U. O.; Wilson, B. R.; Collino, S.; Evans, J. S.; Tamerler, C.; Sarikaya, M., Effect of molecular conformations on the adsorption behavior of gold-binding peptides. *Langmuir* **2008,** *24* (21), 12440-12445.
32. Penna, M. J.; Mijajlovic, M.; Biggs, M. J., Molecular-level understanding of protein adsorption at the interface between water and a strongly interacting uncharged solid surface. *Journal of the American Chemical Society* **2014,** *136* (14), 5323-5331.
33. Rainey, J. K.; Goh, M. C., An interactive triple-helical collagen builder. *Bioinformatics* **2004,** *20* (15), 2458-2459.
34. Monti, S., Molecular dynamics simulations of collagen-like peptide adsorption on titanium-based material surfaces. *The Journal of Physical Chemistry C* **2007,** *111* (16), 6086-6094.
35. Gopalakrishnan, R.; Balamurugan, K.; Singam, E. R. A.; Sundaraman, S.; Subramanian, V., Adsorption of collagen onto single walled carbon nanotubes: a molecular dynamics investigation. *Physical Chemistry Chemical Physics* **2011,** *13* (28), 13046-13057.
36. Morgan, P. H.; Jacobs, H. G.; Segrest, J. P.; Cunningham, L. W., A Comparative Study of Glycopeptides Derived from Selected Vertebrate Collagens A POSSIBLE ROLE OF THE CARBOHYDRATE IN FIBRIL FORMATION. *Journal of Biological Chemistry* **1970,** *245* (19), 5042-5048.

37. Berendsen, H. J.; van der Spoel, D.; van Drunen, R., GROMACS: A message-passing parallel molecular dynamics implementation. *Computer Physics Communications* **1995,** *91* (1), 43-56.
38. Jorgensen, W. L.; Chandrasekhar, J.; Madura, J. D.; Impey, R. W.; Klein, M. L., Comparison of simple potential functions for simulating liquid water. *The Journal of Chemical Physics* **1983,** *79* (2), 926-935.
39. Duke, R.; Giese, T.; Gohlke, H.; Goetz, A.; Homeyer, N.; Izadi, S.; Janowski, P.; Kaus, J.; Kovalenko, A.; Lee, T., AmberTools 16. University of California, San Francisco: 2016.
40. Case, D. A.; Betz, R. M.; Cerutti, D. S.; T.E. Cheatham, I.; Darden, T. A.; Duke, R. E.; Giese, T. J.; Gohlke, H.; Goetz, A. W.; Homeyer, N.; Izadi, S.; Janowski, P.; Kaus, J.; Kovalenko, A.; Lee, T. S.; LeGrand, S.; Li, P.; C.Lin; Luchko, T.; Luo, R.; Madej, B.; Mermelstein, D.; Merz, K. M.; Monard, G.; Nguyen, H.; Nguyen, H. T.; I.Omelyan; Onufriev, A.; Roe, D. R.; Roitberg, A.; Sagui, C.; Simmerling, C. L.; Botello-Smith, W. M.; Swails, J.; Walker, R. C.; Wang, J.; Wolf, R. M.; Wu, X.; Xiao, L.; Kollman, P. A. *AMBER 2016*, University of University of California, San Francisco, 2016.
41. Salomon-Ferrer, R.; Götz, A. W.; Poole, D.; Le Grand, S.; Walker, R. C., Routine microsecond molecular dynamics simulations with AMBER on GPUs. 2. Explicit solvent particle mesh Ewald. *Journal of Chemical Theory and Computation* **2013,** *9* (9), 3878-3888.
42. Maier, J. A.; Martinez, C.; Kasavajhala, K.; Wickstrom, L.; Hauser, K. E.; Simmerling, C., ff14SB: improving the accuracy of protein side chain and backbone parameters from ff99SB. *Journal of Chemical Theory and Computation* **2015,** *11* (8), 3696-3713.
43. Varma, S.; Botlani, M.; Hammond, J. R.; Scott, H. L.; Orgel, J. P.; Schieber, J. D., Effect of intrinsic and extrinsic factors on the simulated D ‐ band length of type I collagen. *Proteins: Structure, Function, and Bioinformatics* **2015,** *83* (10), 1800-1812.
44. Heinz, H.; Lin, T.-J.; Kishore Mishra, R.; Emami, F. S., Thermodynamically consistent force fields for the assembly of inorganic, organic, and biological nanostructures: the INTERFACE force field. *Langmuir* **2013,** *29* (6), 1754-1765.
45. Heinz, H.; Vaia, R.; Farmer, B.; Naik, R., Accurate simulation of surfaces and interfaces of face-centered cubic metals using 12− 6 and 9− 6 Lennard-Jones potentials. *The Journal of Physical Chemistry C* **2008,** *112* (44), 17281-17290.
46. Berendsen, H. J.; Postma, J. v.; van Gunsteren, W. F.; DiNola, A.; Haak, J., Molecular dynamics with coupling to an external bath. *The Journal of Chemical Physics* **1984,** *81* (8), 3684-3690.
47. McQuarrie, D., Statistical Mechanics. *HarperCollins, New York,* **1976**.
48. Ryckaert, J.-P.; Ciccotti, G.; Berendsen, H. J., Numerical integration of the cartesian equations of motion of a system with constraints: molecular dynamics of n-alkanes. *Journal of Computational Physics* **1977,** *23* (3), 327-341.
49. Quan, B. D. Molecular Control of Collagen Biomineralization in the Periodontium. 2015.
50. Huang, C. C.; Couch, G. S.; Pettersen, E. F.; Ferrin, T. E. In *Chimera: an extensible molecular modeling application constructed using standard components*, Pac. Symp. Biocomput, World Scientific: 1996; p 724.
51. Sun, Y.-L.; Luo, Z.-P.; Fertala, A.; An, K.-N., Direct quantification of the flexibility of type I collagen monomer. *Biochemical and Biophysical Research Communications* **2002,** *295* (2), 382-386.
52. Gautieri, A.; Buehler, M. J.; Redaelli, A., Deformation rate controls elasticity and unfolding pathway of single tropocollagen molecules. *Journal of the Mechanical Behavior of Biomedical Materials* **2009,** *2* (2), 130-137.
53. Seker, U. O.; Wilson, B.; Sahin, D.; Tamerler, C.; Sarikaya, M., Quantitative affinity of genetically engineered repeating polypeptides to inorganic surfaces. *Biomacromolecules* **2008,** *10* (2), 250-257.
54. Wang, A.; Vangala, K.; Vo, T.; Zhang, D.; Fitzkee, N. C., A three-step model for protein–gold nanoparticle adsorption. *The Journal of Physical Chemistry C* **2014,** *118* (15), 8134-8142.

55. Willett, R.; Baldwin, K.; West, K.; Pfeiffer, L., Differential adhesion of amino acids to inorganic surfaces. *Proceedings of the National Academy of Sciences* **2005,** *102* (22), 7817-7822.
56. Tang, M.; Gandhi, N. S.; Burrage, K.; Gu, Y., Interaction of gold nanosurfaces/nanoparticles with collagen-like peptides. *Physical Chemistry Chemical Physics* **2018**.
57. Jenkins, C. L.; Raines, R. T., Insights on the conformational stability of collagen. *Natural Product Reports* **2002,** *19* (1), 49-59.
58. Zwillinger, D., *CRC standard mathematical tables and formulae*. CRC Press: 2002.
59. Bodian, D. L.; Radmer, R. J.; Holbert, S.; Klein, T. E. In *Molecular dynamics simulations of the full triple helical region of collagen type I provide an atomic scale view of the protein's regional heterogeneity*, Pacific Symposium on Biocomputing. Pacific Symposium on Biocomputing, NIH Public Access: 2011; pp 193-204.

Table of Content